ORIGINAL ARTICLE

Geophysical and geomorphological approach for locating groundwater potential zones in Sukinda chromite mining area

Ratnakar Dhakate · D. K. Chowdhary ·
V. V. S. Gurunadha Rao · R. K. Tiwary ·
Amlendu Sinha

Abstract The impact of mining causes deterioration of environment and decline of groundwater level in the adjoining mining areas, which influences groundwater source for domestic and agriculture purposes. This necessitated locating and exploiting of new groundwater source. A fast, cost-effective and economical way of locating and exploration is to study and analyze remote sensing data. Interpreted remote sensing data were used to select sites for carrying out surface geophysical investigations. Various geomorphologic units were demarcated, and the lineaments were identified by interpretation of false color composite satellite imageries. The potential for occurrence of groundwater in the Sukinda Valley was classified as very good, good, moderate and poor by interpreting the images. Sub-surface geophysical investigations, namely vertical electrical soundings, were carried out to delineate and demarcate potential water-bearing zones. Integrated studies of interpretation of geomorphologic, lineaments and geophysical data (aquifer thickness) were used to prepare groundwater potential map. The studies reveal that the groundwater potential of shallow aquifers is due to geomorphologic features, and the potential of deeper aquifers is determined by lineaments and degree of weathering.

Keywords Groundwater · Geomorphology · Lineaments and vertical electrical sounding

R. Dhakate (✉) · D. K. Chowdhary · V. V. S. Gurunadha Rao
National Geophysical Research Institute, Uppal Road,
Hyderabad, Andhra Pradesh 500007, India
e-mail: dhakate.ratnakar@gmail.com

R. K. Tiwary · A. Sinha
Central Institute of Mining and Fuel Research, Barwa Road,
Dhanbad, Jharkhand 826001, India

Introduction

In the process of development, mining is one of the core industries contributing, knowingly or unknowingly, toward the deterioration of the environment in terms of air, water and land pollution. To achieve sustainable development, environmental protection elements should be introduced at the planning stage of the mining project. India is endowed with a wide range of mineral reserves. In the country, there are approximately 9,906 mining leases spread over an area of 7,453 square kilometers covering 55 minerals other than fuel (IBM Publication 1997). Metal mining posses problems to the water environment by discharging mine water from underground and open pit mines. Leachate water and run-off water from overburden/waste rock dumps also contaminate nearby water streams (Tiwary et al. 1995; Gajowiec and Witkowski 1993; Godgul and Sahu 1995). The potential impacts from leaching operations on the environment are most likely to be experienced as changes to surface and groundwater quality. The quality of the mine water depends upon various factors including physical characteristics of the ore, net acid generating potential, groundwater characteristics, back fill practice, mining practice and age of mine, etc., and aquifer characteristics.

Level of pollution due to chromite ore mining has also been reported to be severe. In United States, chromites ore is produced around 13 million tons with average grade (30%) and produces 9 million ton waste. Tailing dam's seepage as well as effluent discharged from concentration and screening plants also plays an important role in groundwater pollution. The surrounding soil and plants are also reported to be enriched in chromium content around the chromium-rich ultramafic terrains in Pakistan (Kafay yatullah). Previous studies have shown that a high degree of heavy metal contamination in soil and plants has

occurred in many places in the world, which could be related to the occurrence of ore deposits (Gough et al. 1989).

The Sukinda Valley in Jajpur District, Orissa, is known for its deposit of chromites ore producing nearly 8% of chromite ore in India. There are number of open cast mines in the area. During the process of mining, the waste rock materials as well as chromite ores are dumped on ground surface. In Sukinda mining area, around 7.6 million tones of solid waste have been generated in the form of rejected minerals, overburden material/waste rock and sub-grade ore (IBM Publication 1997). The mine seepage water is also discharged into the nearby drainage, which is often being used as source of water by adjoining villages.

Chougule (1981) have carried out systematic hydrogeological investigations in parts of Salandi-Battarani and Brahmani River Basin. Das and Kar (1997) also carried out hydrogeological investigations in Sukinda Valley with special reference to mining activities. They have concluded their studies that the groundwater occurs under phreatic conditions. Groundwater is a primary source of fresh water in this region. There has been a growing demand for fresh water for various purposes, such as domestic, agricultural and industrial use. In order to meet the demand, the delineation of potential groundwater zones is essential. There have been several methods such as geophysical and geological methods to delineate groundwater potential zones. However, many of these methods are costly and time-consuming. The main source of potable water in the area is groundwater, which is tapped by shallow dug wells, and deep bore wells. In order to protect groundwater from the contamination of chromite, it is vital to understand the hydrogeology and its characteristic parameters. Detail geophysical studies have been carried out to understand the hydrogeological settings and aquifer behavior in and around the mining area.

In recent years due to the advancement in technology, most scientists and researchers are taking the help of current technology for planning, monitoring and decision-making. Remote sensing is one such technology that is very useful for agricultural scientists and other researchers to locate groundwater. Using this technology, different thematic maps are generated such as soil cover maps, lineament maps and geomorphologic maps. These maps are useful for groundwater studies and reduce the additional expenditure and personnel required for further exploration (Yadav and Lal 1989; Bhimasankar et al. 1970; Bhimasankarm and Gaur 1977).

Lineament analysis followed by resistivity survey is cost effective while studying geomorphologic data. In order to assess the groundwater conditions in the area, electrical resistivity surveys were carried out with Schlumberger electrode configuration to pinpoint the most favorable locations in the area. Integrating hydrogeomorphological data with geophysical investigations Teeuw (1999), Shahid and Nath (2002), Srivastava and Bhattacharya (2006), Dhakate et al. (2008) have evolved a simple and rapid approach for demarcation of groundwater potential. The objective of the present study is to demarcate the groundwater potential zones in and around the mining lease areas. This will facilitate the mapping and prevention of groundwater from pollution especially from hexavalent chromium if any occurred in and around the mining areas.

Study area

In order to study the hydrogeological settings in a typical chromite open cast mining area, about 106 sq km has been selected in the Jajpur District, Orissa, India, which forms a part of Sukinda Valley as shown in Fig. 1. Drainage in the area is toward NW, which finally join Damasal Nala. Damasal Nala is perennial in nature as most of the mine seepage is discharged into it. In the south, the Mahagiri Hill ranges have an altitude of 400 m above mean sea level, and in the north, Daitri Hill ranges have an altitude of 200 m above mean sea level, whereas the elevation of Damasal Nala and its surrounding occur between 100 and 180 m above mean sea level. The various active mining lease areas for different companies are shown in Fig. 2.

Geological background

The chromites deposits form a part of famous chromite bearing ultramafic complex of Sukinda Valley. These ultramafics are highly metamorphosed and belong to Pre-Cambrian age. The rocks of the area are associated with six sedimentary sequences, and each is separated by unconformities (Banerjee 1971; Acharya et al. 1998). The Sukinda ultramafic complex is bounded in the north by the Daitari Hill range and in the south by the Mahagiri Hill ranges, which are mostly composed of quartzites. The general trend of the Daitari Hill is E–W, while that of Mahagiri Hill is NE–SW. The Sukinda Valley presents a synformal fold plunging toward WSW at a low angle, 10°–15° (Banerjee 1971). The ultramafics appear to have been intruded into the quartzites, and this layered laccolithic complex is composed of alternate bands of chromite, dunite, peridotite and orthopyroxenite, repeated in a rythimic fashion. These ultramafics are extensively lateritized and limonitized. The occurrences of numerous chert bands are also found within the ultramafics, which are often completely weathered to a mass of talc–limonite. The chromite ores occur as bands within the ultramafic body at six stratigraphic levels. The thickness of chromite ore body

Fig. 1 Key map showing the geology of the study area
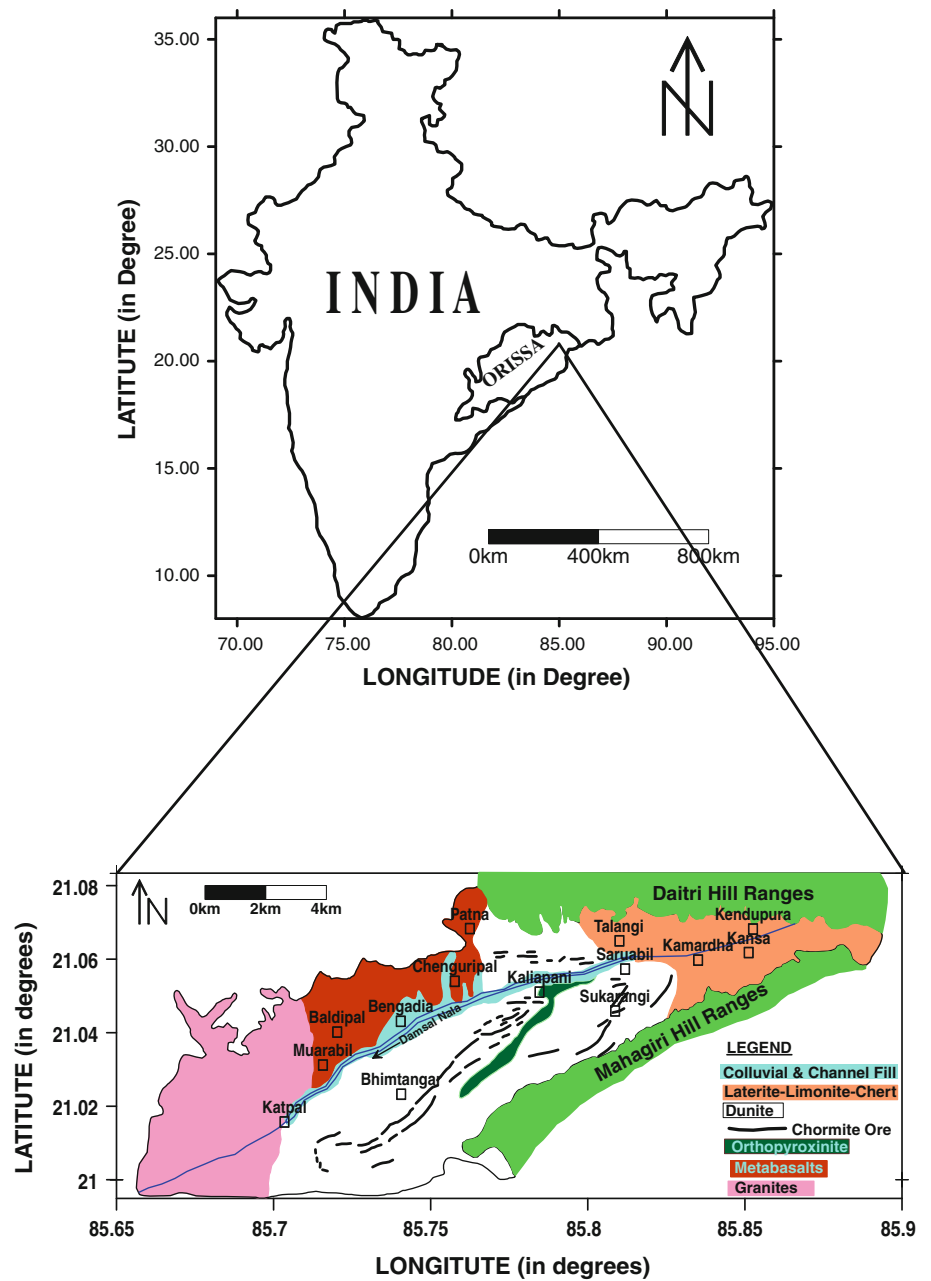
Fig. 2 Different mining location lease to various companies
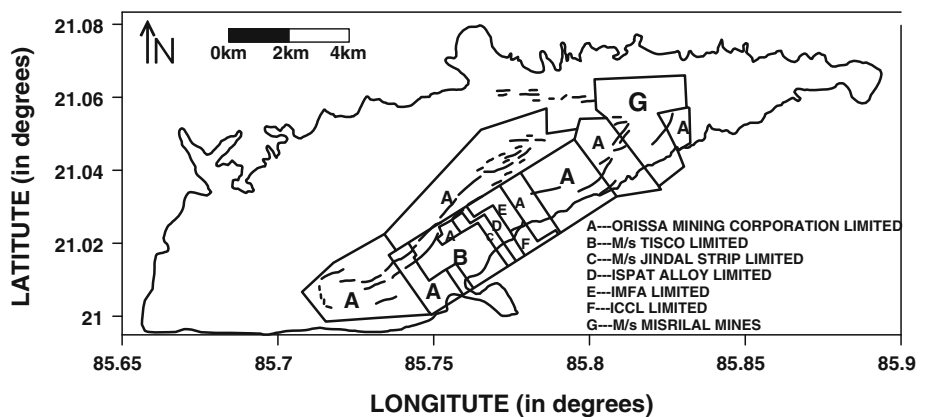
Table 1 Stratigraphy of the Sukinda chromite mining area

Age		Lithology
Recent to Pleistocene		Soil, alluvium laterite
Unconformity		
Precambrian	Ultramafic	Dolerite
		Granite
		Gabbro-diorite
		Pyroxenite
		Dunite
		Peridotite with chrome ore
	Meta-sediments and	Gritty-quartzite
	Meta-volcanics	Meta-volcanics
Base not seen		

ranges from 0.3 to 20 m and in length from 100 m to 7 km. The thickest and longest bands occur in Kaliapani–Bhimtanagar tract, whereas, in the western sectors, the ores occur as dissemination or discontinuous bands. In the east, the ores are friable to lumpy in nature. The geological map of the study area is shown in Fig. 1. The stratigraphy of the areas is given in Table 1.

Hydrology of the area

The weathered lateritized–limonite mantle, ultramafics, orthopyroxenite, as well as the underlying semi-weathered and fractured country rocks, form the source of groundwater in the area (Chougule 1981; Das and Kar 1997). The groundwater occurrence depends on the nature and the extent of weathering characteristics of the rock formation. The groundwater in the area is generally under semi-confined to confined condition. The various hydrogeological units are as follows.

Laterite–Limonite–Chert

These are the altered product of ultramafics. These are the most extensive and potential aquifers and occur in the eastern part of the area (Chougule 1981; Das and Kar 1997). The groundwater in this zone occurred in the upper part of aquifer (up to 25 m) under the phreatic condition, whereas the deeper aquifer occurs (below 25 m) under confined condition. The seasonal fluctuation of water level in this formation is very low.

Laterite-weathered and fractured ultramafics associated with limonite and chert

This formation occupies the central and west central parts and covers almost the entire mining tract in the Sukinda

Valley. The formation lies below a thin and discontinuous capping of the soil and lateritic mantle, which persists up to a depth range of 20 m. The extent of weathering in this formation is comparatively less than the laterite–limonite–chert formation. The groundwater occurs in this formation is under phreatic condition up to a depth of 20–25 m bgl (Chougule 1981; Das and Kar 1997). The deeper aquifer in this formation constituted by the weathered–semi-weathered and fractured ultramafics generally remains in hydraulic continuity with top aquifer, and groundwater generally exists in these deeper horizons near to water table conditions.

Colluvial and channel fill deposits

This formation is generally the mixture of boulders, gravels, pebbles, granules, etc., which is highly cemented with ferruginous and siliceous matrix, and have restricted occurrences in the foot hill of Mahagiri and Daitri Hill ranges region and along the course of Damasal Nala. The maximum thickness of this formation is around 12–15 m (Chougule 1981; Das and Kar 1997). The average seasonal fluctuation of water level in this formation is around 4 m.

Other hydrogeological units including orthopyroxenites

This group of formations includes orthopyroxenites occurring in the central part around Purnapani village. These formations except the orthopyroxenites are comparatively less weathered, and maximum thickness of weathering is up to 15 m bgl (Chougule 1981; Das and Kar 1997), whereas orthopyroxenites from low-ridge-like exposures and extend of weathering is maximum up to a depth of 10 m.

Geophysical investigation

The geophysical data of vertical electrical sounding (VES) used in the paper are namely acquired by surface investigations. Hence, the relevant information of the same is discussed. Moreover, among all the surface geophysical techniques for groundwater prospecting, Electrical Resistivity Method is the most widely applied method all over the globe. This is because of its efficacy to detect the water-bearing layers, besides being simple and inexpensive to carry out the field investigations (Zohdy 1974). Due to the above factors, the VES surveys are still preferred to carry out for groundwater prospecting. The VES measures the parameters of resistivity at various depths in the subsurface.

In general for measuring the resistivities of the subsurface formations, four electrodes are required. A

current of electrical intensity (*I*) is introduced between one pair of electrodes, called current electrodes. The current electrodes can be identified as A and B and sometimes $+I$ and $-I$ denoting source and sink, respectively. The potential difference produced as a result of current flow is measured with the help of another pair of electrodes, called potential electrodes or probes. The potential electrodes may be represented as M and N. If ΔV represents the potential difference, then the apparent resistivity is given by 'G' ($\Delta V/I$), where 'G' is geometrical constant. Schlumberger array has been adopted to carry out VES.

Schlumberger array

This array uses four collinear point electrodes, but measures the potential gradient at the mid-point by keeping the measuring electrodes close to each other. Four electrodes are placed along a straight line symmetrically over center point 'O'. Current (*I*) is sent through the outer current electrodes *A* and *B*, and the potential is measured across inner potential electrodes *M* and *N*. The separation between the potential electrodes is kept small when compared to the current electrodes separation. The separation chosen is such that for all measurements ($MN < 1/5AB$). The most common spacing of $AB/2$ (current electrode) and $MN/2$ (potential electrodes) chosen for carrying out VES by using Schlumberger Configuration is for current electrodes $AB/2 = 1.5, 2.0, 2.5, 3.0, 4.0, 5.0, 6.0, 8.0, 10, 12, 15, 20, 25, 30, 40, 50, 60, 70, 80, 90$ and 100 m and so on. For potential electrodes, $MN/2$ spacing is 0.5, 2.0, 5.0 and 10 m and so on. The configuration or geometric factor for the Schlumberger array is given by $G = \frac{(AB/2)^2 (MN/2)^2}{(MN/2)} \frac{\pi}{2}$.

Where *AB* is the distance between current electrodes, *MN* is the distance between potential electrodes, and the apparent resistivity is obtained with the formula $\rho_a = G (\Delta V/I)$, where ($\Delta V/I$) is the potential difference between potential electrodes to that of current flowing.

Depending upon the apparent resistivity values, the observed ΔV and I increase or decrease with each electrode separation. The observed apparent resistivity (ρ_a) values are plotted on a double log graph. Half current electrode separation is plotted on *X*-axis and the corresponding apparent resistivity (ρ_a) on *Y*-axis. The plotted points are joined to draw a curve. This is called the sounding curve. The shape of the curve changes, and this curve is helpful for the quantitative interpretation of the electrical resistivity data. The qualitative interpretation of the sub-surface layer resistivity distribution can be observed from the shape of the curve. The sounding curve is interpreted by matching the same with master curves of two-, three- and four-layer cases for various ratios of absolute resistivity

given (Orellena and Mooney 1966). The three-layered earth model can be classified into A, Q, H and K type curves based on the shape. Similarly, four-layer curves are AA, QQ, HK, KH, HA, KQ, AK, QH and five-layer curves area AAA, HAA, HKH, and KHK, etc.

Depending upon whether apparent resistivity values increases or decreases with each electrode separation, the shape of the curve changes and this curve is helpful for quantitative interpretation of the electrical resistivity data. The qualitative interpretation of the sub-surface layer resistivity distribution can be observed from the shape of the curve. A curve is drawn by plotting the observed apparent resistivity (ρ_a) values against the current electrode separation ($AB/2$) on a log–log graph sheet, and this is interpreted by matching the field curve with master curves of two-, three- and four-layer cases for various ratios of absolute resistivity given by (Orellena and Mooney 1966). The interpretation of resistivity sounding curve has been carried out through Master Curves (Orellena and Mooney 1966) and iterative inversion method (Jupp and Vozoff 1975) to arrive more accurate interpretation results. A summary of the interpreted results of VES is given in Table 2. The location of VES along with geomorphological map is shown in Fig. 3. The resistivity ranges of various litho-units are given in Table 3.

From resistivity survey, it is found that the depth of aquifer varies from 4 to 40 m below ground level and there exists two aquifer systems in the area, one at a depth of 0–25 m below ground level in unconfined condition and another at a depth of 25–60 m below ground level in confined condition (Rao et al. 2002). The aquifer that occurs at a depth of 0–25 m bgl has thickness ranging from 1 to 26 m, and the aquifer that occurs at a depth of 25–60 m has thickness ranging from 2 to 40 m. Along the foot hills, the thickness of an aquifer is shallow, whereas in the central part of the area, the thickness of aquifer is more. Similarly, the depth to shallow aquifer is more in central, northern and south-eastern part of the area, whereas the depth to deeper aquifer is more in central part of the area. The spatial variation of shallow and deeper aquifer thickness is shown in Fig. 4a, b.

Geomorphology

The study area has a peneplained topography with an elevation that ranges from 80 to 100 m. Two main ridges, the Daitari and the Mahagiri, trend NE–SW with an intervening valley fill. Damasal, the major river in the area, flows westward. LANDSAT TM false color composite (FCC) of bands 2, 3 and 4 for the year 1997 of Sukinda Valley was used to identify the following geomorphologic units by visual interpretation (Subramanyam

Table 2 Interpreted results of vertical electrical sounding carried out in Sukinda area

VES no	ρ_1	ρ_2	ρ_3	ρ_4	ρ_5	ρ_6	h_1	h_2	h_3	h_4	h_5	Total H
1	21	42	7	76	384	–	1.0	3.6	13.1	7.6	–	25.4
2	191	227	206	540	77	–	1.7	4.9	24.3	11.6	–	42.5
3	176	78	258	700	–	–	0.7	4.2	5.1	–	–	10.1
4	548	1,625	2,327	93	–	–	0.7	6.5	14.3	–	–	21.5
5	6,575	1,058	303	127	–	–	2.1	7.9	7.8	–	–	17.8
6	296	142	313	833	307	–	0.6	1.1	8.9	11.6	–	22.2
7	256	27	265		–	–	0.6	2.8		–	–	3.5
8	161	175	277	52	–	–	1.1	10	14	–	–	25.3
9	436	996	189	46	–	–	0.8	3.9	14.5	–	–	19.2
10	250	423	94	10	177	–	0.9	4.7	6.1	18.2	–	30
11	2,950	3,416	505	43	–	–	1.4	3.5	8.6	–	–	13.4
12	51	10	5	138	–	–	2.2	2	16.9	–	–	21.1
13	173	483	21	59	81	–	2.2	4.7	12.9	15.8	–	35.5
14	34	7	28	90	–	–	0.6	4.6	17.8	–	–	23.1
15	272	5,743	254	316	951	91	0.6	2.3	7.9	2.9	23.8	37.5
16	238	1,333	483	227	–	–	0.8	9.5	24.1	–	–	34.3
17	856	151	1,973	68	–	–	0.7	1.8	6.7	–	–	9.2
18	1,134	177	12	68	–	–	1.9	3.8	16	–	–	21.8
19	7	76	17	138	–	–	1.1	7.9	16.6	–	–	25.7
20	934	2,049	381	81	–	–	0.7	1.8	35.5	–	–	38.1
21	47	9	37	84	–	–	0.9	5.8	13.2	–	–	19.9
22	44	21	7	270	–	–	0.6	6.3	10.3	–	–	17.1
23	97	15	41	173	–	–	0.6	9.8	10.3	–	–	20.7
24	1,950	4,435	357	22	166	–	0.8	2.6	12.2	22.4	–	38
25	103	2,043	174	530	–	–	0.7	4.3	15.9	–	–	20.9
26	121	117	32	1,780	–	–	1.1	3.4	6.9	–	–	11.4
27	455	1,978	413	76	–	–	1.5	11	9.5	–	–	21.7
28	145	40	450	8	303	806	0.5	1.1	3.6	17.1	8.9	31.2
29	59	16	426	70	–	–	0.6	1.6	10.2	–	–	12.5
30	629	2,776	588	230	–	–	1.2	15	17	–	–	32.7
31	184	94	900	7,943	65	–	0.7	1.2	1.3	9	–	12.3
32	474	2,310	141	56	–	–	0.9	3.8	15.6	–	–	20.4
33	20	8	51	859	–	–	0.5	4.4	9.4	–	–	14.4
34	39	52	549	23	–	–	1	1.1	4.9	–	–	6.9
35	147	1,604	89		–	–	2.8	3.9		–	–	6.7
36	179	244	8	120	–	–	1.2	4.9	16.3	–	–	22.4
37	198	169	63	716	–	–	1	4.5	12.4	–	–	17.8
38	589	463	33	62	–	–	1.6	8.7	30.4	–	–	40.7
39	336	22	261	8,321	–	–	1.3	5.5	4.1	–	–	10.9
40	65	72	215	919	–	–	0.9	1.8	14.7	–	–	17.4
41	66	72	41	271	–	–	0.9	4.5	7.9	–	–	13.4
42	118	143	13	998	–	–	1.3	5.8	11.4	–	–	18.4
43	273	370	57	609	–	–	0.8	5.2	16.8	–	–	22.8
44	380	250	57	606	–	–	0.8	7	19	–	–	26.8
45	280	534	51	11	–	–	2	10	8.7	–	–	20.9
46	18	5	43	409	–	–	2.4	8.2	4.5	–	–	15.1
47	165	35	254	846	1,470	–	1.5	3.3	3.6	7.5	–	15.9
48	31	251	290	317	–	–	0.8	4.2	8.9	–	–	13.8

Table 2 continued

| VES no	ρ_1	ρ_2	ρ_3	ρ_4	ρ_5	ρ_6	h_1	h_2	h_3	h_4	h_5	Total H
49	932	84	1,088	22	–	–	0.8	2.9	12	–	–	15.6
50	21	5	78	106	–	–	0.7	3	15.9	–	–	19.5
51	261	34	9	184	–	–	0.6	3.6	21.1	–	–	25.3
52	61	315	28	143	–	–	1.4	7.1	20.5	–	–	29
53	422	191	91	2,048	–	–	0.6	6.2	12	–	–	18.9
54	1,026	453	115	603	–	–	0.6	9.2	13.2	–	–	23
55	214	1,486	129	569	81	–	2.1	2.3	3.4	4.4	–	12.2
56	562	2,529	133	96	–	–	1.5	4.0	25.9	–	–	31.4
57	320	1,812	206	25	–	–	1.0	7.0	4.0	–	–	12
58	374	197	144	47	–	–	3.6	6.2	22.6	–	–	32.4
59	318	78	387	55	–	–	0.6	3.4	22.0	–	–	26
60	456	141	51	453	–	–	0.9	12.2	40.7	–	–	53.8
61	561	190	2,614	301	–	–	0.7	1.6	11.6	–	–	13.9
62	445	106	384	52	–	–	0.6	2.7	12.2	–	–	15.5
63	93	2,226	156	51	–	–	0.8	5.0	21.9	–	–	27.7
64	47	14	74	9,674	–	–	0.8	2.4	31.3	–	–	34.5
65	95	8.0	8,816	–	–	–	0.9	11.6	–	–	–	12.5
66	567	398	6,344	62	5,009	501	1.3	2.5	15.0	14.7	12	33.5
67	634	2,241	547	11	–	–	0.7	2.8	9.5	–	–	13
68	232	12	10,069	–	–	–	6.0	30.7	–	–	–	36.7
69	407	1,610	40	–	–	–	1.5	10.5	–	–	–	12
70	16	6	38	9,920	–	–	0.9	4.3	30.4	–	–	35.6
71	544	286	2,303	537	204	–	0.8	1.0	10.6	31.3	–	43.7
72	181	114	12	10,060	–	–	1.0	6.1	20.1	–	–	27.2
73	10	155	649	205	–	–	1.5	10.2	32.6	–	–	44.3
74	364	113	42	9,998	–	–	1.8	28.5	42.1	–	–	72.4
75	336	652	126	240	–	–	0.8	1.8	20.2	–	–	22.8
76	346	813	100	19	10,094	–	0.6	3.3	11.2	33.1	–	48.2
77	130	314	9.0	10,434	–	–	1.0	1.8	11.1	–	–	13.9
78	32	11	60	23	10,217	–	1.0	14.1	11.8	11.3	–	38.2
79	265	27	119	–	–	–	0.6	5.0	–	–	–	5.6
80	15	13	65	9,996	–	–	1.6	1.4	58.0	–	–	61
81	343	115	468	52	–	–	0.7	1.4	4.9	–	–	7

Fig. 3 Geomorphological map showing vertical electrical sounding locations and geophysical cross sections
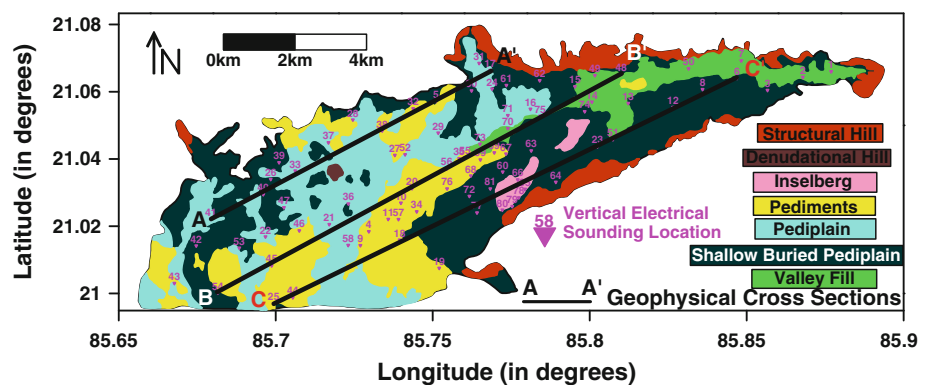
Table 3 Resistivity ranges of various litho-units

Litho-units	Resistivity (Ohm-m)
Clay	<10
Sandy clay/clayey sand and kankar (Aquifer)	10–25
Weathered dunite/peridotite/metabasalt (Aquifer)	>25–160
Hard and massive bed rock	>160

described below. Such studies have been carried out in different parts of India by Haridas et al. (1994); Dubey and Trivedi (1994); Lokesh and Narayana (1996); Palanivel et al. (1996); Sree Devi et al. (2001); Dhakate et al. (2008). The various geomorphologic units identified are shown in Fig. 3, and a brief summary of each geomorphologic unit for groundwater prospects is given in Table 4.

Structural hills

These are linear to curvilinear landforms characterized by their high relief, steep slope and parallel drainage pattern.

1986). The landform identified from the satellite images is helpful in identifying favorable zones for groundwater (Thornburry 1969). The various geomorphologic units identified using FCC for interpretation are defined and

Fig. 4 **a**, **b** Variation of aquifer thickness for shallow and deeper aquifer
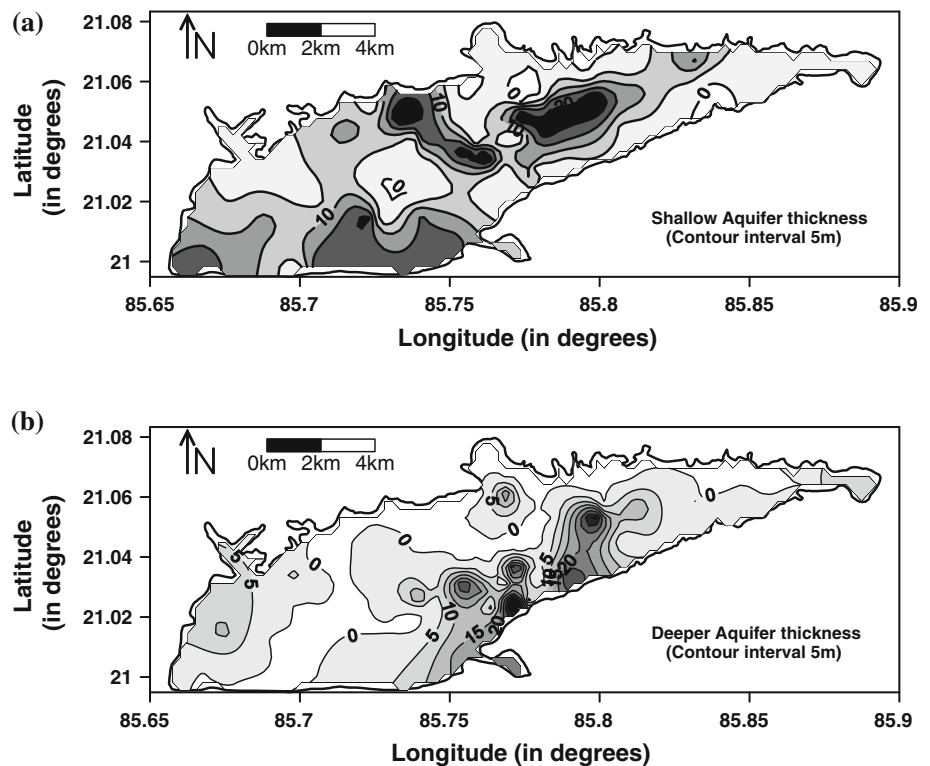
Table 4 Description of geomorphological units along with groundwater prospects

Land forms	Description	Groundwater prospects
Structural hill	Linear to curvilinear landforms with high relief, steep slopes and parallel drainage	Poor
Denudo-structural hill	Dissected hills having a linear trend along with rounded to sub-rounded crests and rugged topography	Poor
Residual hill	Isolated hillocks with dark tone	Poor
Pediment	Erosional land with breaks of slope and lighter to medium gray tone	Moderate to poor
Peneplain	Reddish color with relatively low elevation	Moderate
Shallow buried pediplain	Land use pattern with white to grayish white color and low drainage density	Moderate to good
Valley fill	Vicinity of streams with very light gray tone	Very good

In the FCC, these are identified by alternating ridge and valley topography and moderate to dense vegetation cover.

Denudational hills

These are highly dissected hills having a nearly linear trend. These are characterized by rounded to sub-rounded crests and rugged topography. Effect of leaching and weathering is quite conspicuous in these units.

Pediments

This erosion land unit is associated with breaks of slope and comprises of mainly floats. In the FCC, its lighter to medium gray tone can very well delineate this unit.

Peneplain

This unit is well identified by its reddish color with smooth surface of relatively low relief and elevation. In the Sukinda Valley, this unit carries lateritic cover, which may be regarded as the duricrust.

Shallow buried pediplain

It is characterized by white to grayish white color. The major bulk of it forms the residual soil and alluvial cover. The land use (cultivated lands) and a very low drainage density are the other factors that help to identify this unit.

Inselbergs

These are mostly barren, rocky, and usually smooth and rounded small hills structures. The groundwater is very poor as they will not hold or transmit water and acts as run-off zones.

Valley fills

These are the areas delineated in vicinity of the streams having a very light gray tone and occur as narrow belts along the streams. In addition to all these landforms, features like springs, ridge crest, physiographic trends, etc. have also been mapped. The springs are identified by presence of wetlands, moisture and greenness indices from satellite imagery.

Lineaments

The river Damasal flows along the axis of the plunging syncline and forms one of the most prominent linear features of the study area. The lineament map shows three distinct trends, namely ENE–WSW, N–S and NW–SE as shown in Fig. 5. The lineament density map shows lower range of values for the valley, that is, the chromite bearing lateritized ultramafics (0.0–0.8 km/sq km), while quartzites show a higher range up to 2 km/sq km. Lineaments are linear features of tectonic origin that are long, narrow and relatively straight alignments visible in satellite images due to tonal differences compared to other terrain features. A lineament may represent a fracture (fault and/or joint). It is a long and linear geological structure that may be represented on satellite images as a straight course of streams, vegetation alignment or topographic features such as aligned ridges. The lineaments observed in the study area may be the results of faulting and fracturing, and hence it is inferred that these are zones of increased porosity and permeability in the hard rock areas. Lineament studies are significant in groundwater prospecting, and remote sensing data provide useful information to identify such structural features. The lineaments were identified by visual interpretation of satellite imageries, using FCC of Thematic Maps (TM Data) of the study area. Similarly, the number of major and minor lineaments is identified from the satellite imagery as shown in the lineament map of the study area in Fig. 5. The lineaments identified are of varying dimensions with different orientations. From resistivity surveys, it is found that in areas where lineaments are intersecting, the thickness of weathering increases. These are, therefore, potential areas for the occurrence of groundwater. A rose diagram of lineaments is shown in Fig. 5 along with lineament diagram. The figure shows that majority of the lineaments shows ENE–WSW, N–S and NW–SE trends.
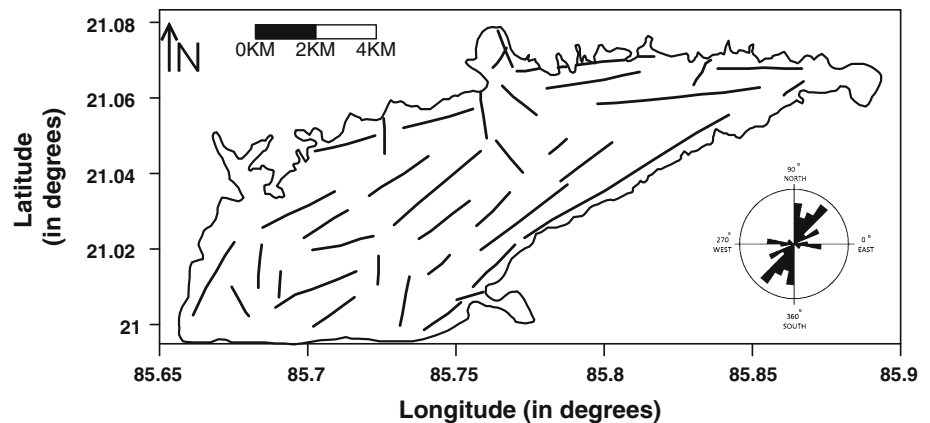
Lineament density map

The lineaments present in the study area have varying dimensions. Based on the concentration and length of lineaments, a lineament density map was prepared. The lineament map as shown in (Fig. 5) was superimposed on a grid map of 1.1 cm by 1.1 cm (2 km by 2 km), and the total length of lineaments passing from each of grid was measured and plotted in the respective grid centers. The values obtained for each grid were interconnected by isolines and based on the concentration and length of lineaments, a lineament density map was prepared as shown in Fig. 6. Lineaments are the main features that control the occurrence of groundwater and are the weak zones where accumulation occurs.
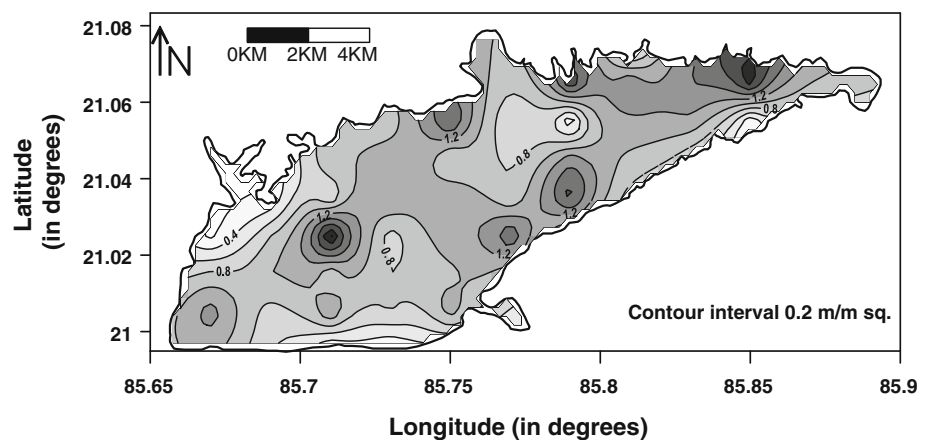
Results, discussion and interpretation

Eighty-one VES using Schlumberger configuration with 100 m half current electrode separation (AB/2) were

Fig. 5 Lineament and rose diagram map of the study area

Fig. 6 Lineament density map of the study area

carried out. The location of these VES is shown along with the geomorphologic map of the area in Fig. 3. The VES data are first interpreted using the curve matching technique (Orellena and Mooney 1966) and then by Inversion Iteration Method (Jupp and Vozoff 1975). The interpreted results of VES are given in Table 1. Based on interpreted results of VES, following resistivity ranges of different sub-surface layers are calculated and given in Table 2. After analyzing the resistivity data interpretation, it is found that the resistivity of the aquifer zone ranges from <10 to 160 Ohm-m for shallow and deeper aquifer. A map showing the spatial variation in the thickness of shallow and deeper aquifer zone is shown in Fig. 4a, b.

Four sounding curves occur in Inselberg geomorphological units. Out of these, 1 curve shows 3-layer H-type curve, 2 curves show 4-layer with HA type and HK type and 1 curve shows 5-layer HKH type

Twenty-five sounding occur in Pediments geomorphological units. Out of these, 3 curves show 3-layer cases (1 curve is of H type and the other two of K-type), 18 curves show 4-layer cases (1 curve is of HA type and HK type, 2 of AK type and KH type, 3 of QH type and 9 curves of KQ type), 3 curves show 5-layer cases (1 curve of KHK type

and 2 curves of KQH type) and 1 curve shows 6-layer case (1 curve of HKHA type).

Thirteen sounding curves occur in Pediplain geomorphological units. Out of these, 11 curves are of HA, QQ, KQ, QH, and HK, KH types showing 4-layer sounding case (1 each sounding curves is of QQ, KQ and HK types, 2 of HA type and QH type, while 4 sounding curves of KH type cases) and 2 curves are of HAK type and HKQ type showing 5-layer cases.

Thirty sounding curves occur in shallow buried pediplain geomorphological units. Out of these, 1 curve shows 3-layer H type, 24 curves show 4-layer sounding curves (1 is of AK type and QQ type, 2 of KQ and AA type, 3 of HK type and 4 of HA type and KH type, while 7 curves show QH type), 4 curves show 5-layer sounding curves (1 each is of KHA, HAK, KQH and HAA types) and 1 shows 6-layer sounding curve of KHAK type).

Nine sounding curves occur in Valley Fill geomorphological units. Out of these, 1 curve is of H-type 3-layer curve, 6 curves show 4-layer (1 curve is of KH, HK, AK and HQ types and 2 of HA type) and 2 curves show 5-layer cases (1 each shows KHA type and KHK type). The analysis of sounding curve (VES No.) with geomorphology unit is

Table 5 Analysis of VES with geomorphological units

Geomorphological unit	Curve type	Nos. of layers	VES nos.
Inselberg	H	3	65
	HA	4	80
	HKH	5	78
	HKHK	6	66
Pediments	H	3	68
	K	3	35, 69
	HA	4	46
	AK	4	4, 34
	KQ	4	9, 11, 20, 27, 32, 45, 56, 57, 67
	QH	4	18, 38, 44,
	HK	4	59
	KH	4	19, 25
	KHK	5	55
	KQH	5	10, 76
	HKHA	6	28
Pediplain	HA	4	21, 33
	QQ	4	58
	KQ	4	16
	QH	4	22, 37
	HK	4	17
	KH	4	29, 41, 43, 52
	HAK	5	31
	HKQ	5	71
Shallow buried pediplain	H	3	79
	HA	4	3, 23, 39, 64
	AK	4	8
	QQ	4	5
	KQ	4	30, 63
	QH	4	12, 51, 53, 54, 60, 72, 74
	HK	4	61, 62, 81
	KH	4	26, 36, 42, 77
	AA	4	40, 48
	KHA	5	13
	HAK	5	6
	KQH	5	24
	HAA	5	47
	KHAK	6	15
Valley fill	H	3	7
	KH	4	75
	HA	4	14, 50
	HK	4	49
	HQ	4	70
	AK	4	73
	KHA	5	1
	KHK	5	2

given in Table 5. A sample of four- and five-layer sounding curve for pediments, pediplain, shallow buried pediplain and valley fill geomorphologic units is shown in Fig. 7a–d.

Three geophysical cross sections are shown in Fig. 8a–c, correspond to different geomorphological units. The A–A' geophysical cross section is drawn by using the sounding
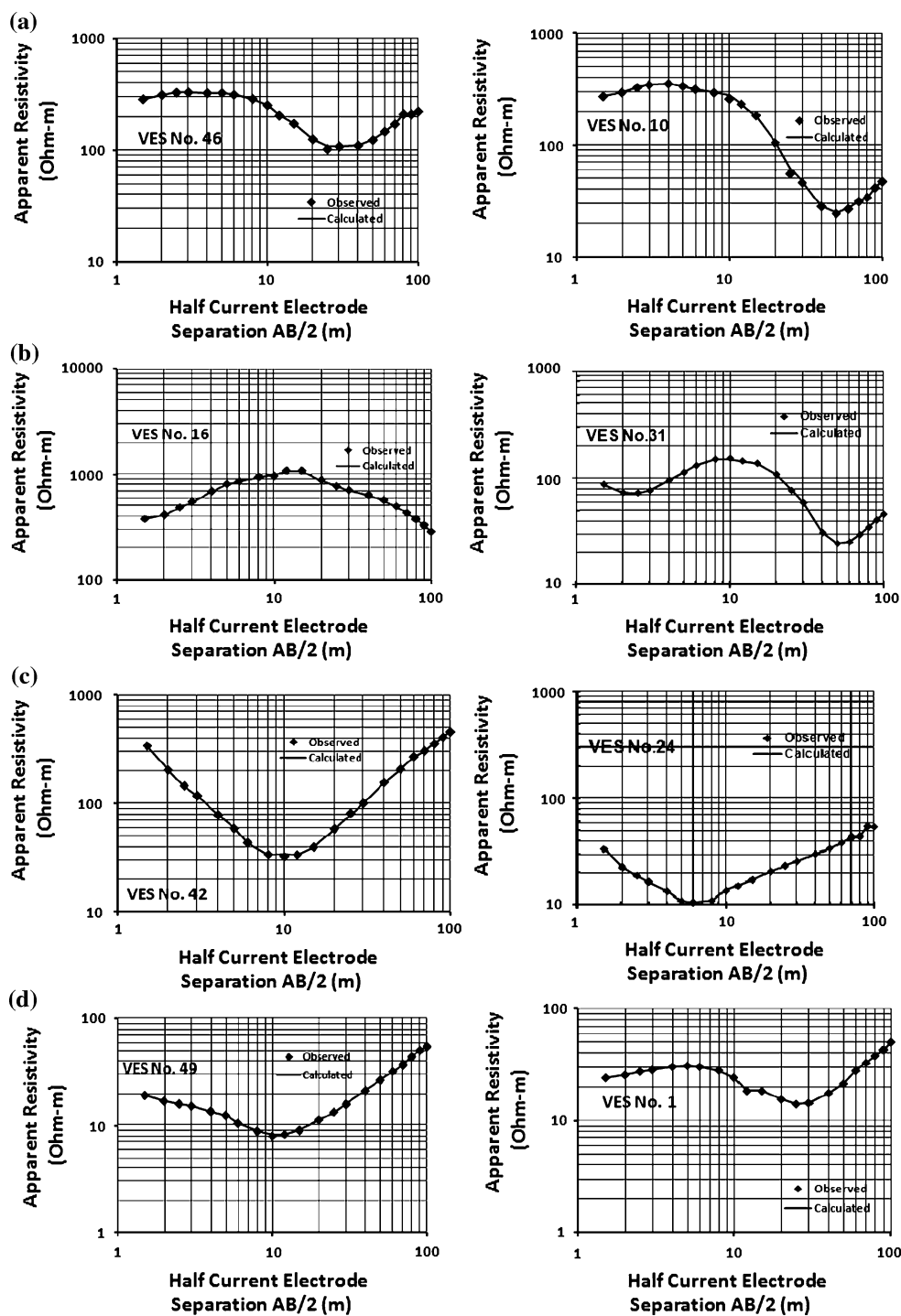
Fig. 7 Vertical electrical sounding curves for **a** pediments, **b** pediplain, **c** shallow buried pediplain and **d** valley fill

curves 41, 40, 33, 38, 32, 5 and 17, respectively. In cross section, A–A' sounding nos. 33, 38, 32 and 17 falls in pediment geomorphologic unit show weathering thickness 9.4, 30.4, 15.6 and downward and 1.8 m and downward, respectively, two sounding 40 and 5 falls in shallow buried pediments show weathering thickness 1.8 and 21.5 m and downward, respectively, and one sounding 41 fall in

pediplain shows weathering thickness 12.4 m. B–B' geophysical cross section is drawn by using sounding curves 54, 45, 21, 20, 35, 73, 70, 75 and 48, respectively. Sounding nos. 45, 20 and 35 falls in pediments unit with weathering thickness 8.7 and downward, 39.1 and 3.5 m and downward, two sounding nos. 54 and 48 falls in shallow buried pediplain with weathering thickness 13.2 m
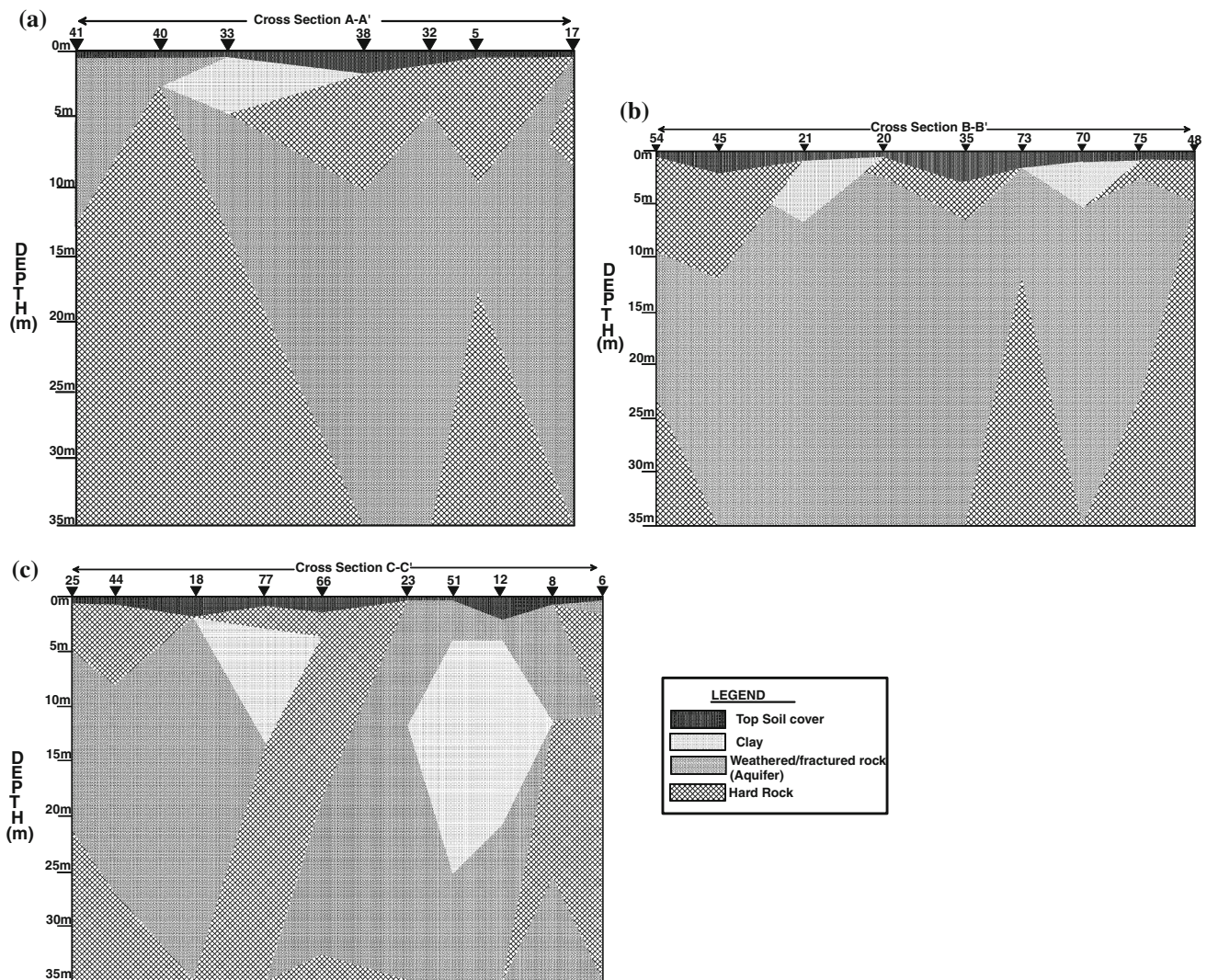
Fig. 8 **a–c** Geophysical cross sections (A–A′, B–B′ and C–C′)

only at sounding no. 54 and sounding no. 48 do not show any weathering, three sounding nos. 73, 70 and 75 falls in valley fills units with weathering thickness 10.2, 30.4 and 20.2 m, respectively. In sounding no. 70, clay layer of thickness 4.3 m is found at depth 0.9 m, which is deposited by run-off sedimentation and its presence for groundwater occurrence is neglected due to the more thickness of weathering at this point. One sounding no. 45 is fall in pediment unit with weathering thickness 8.7 m and downward weathering. C–C′ geophysical cross section is drawn by using sounding curves 25, 44, 18, 77, 66, 23, 51, 12, 8 and 6, respectively. Sounding nos. 25, 44 and 18 falls in pediment unit, the weathering thickness at these soundings is 15.9, 1.9 and 16 m and downward weathering, respectively. Sounding nos. 77, 23, 51, 12, 8 and 6 falls in shallow buried pediplain unit. At sounding no. 77, clay layer is encountered with thickness 11.1, which is a local

phenomenon, and its role in groundwater prospects can be neglected, while at other sounding curves, good weathering thickness occurs. Sounding no. 66 fall in Inselberg unit with weathering thickness 14.7 m. Each geophysical cross section is drawn using different VES located in different geomorphological units, which shows the variation in thickness of aquifer zone, and differs from curve type to type. These three cross sections are shown in Fig. 8a–c, respectively.

Based on the resolution of interpreted VES data, a map showing the spatial variation in the thickness shallow and deeper aquifer zone is shown in Fig. 4a, b. The thickness of shallow and deeper aquifer is classified into three groups. Area showing the aquifer thickness less than 5 m is classified as poor, whereas showing aquifer thickness 5–10 m is classified as moderate. Similarly, the area that shows the aquifer thickness 10–15 m is classified as good, and the

Fig. 9 Groundwater prospect map of the area
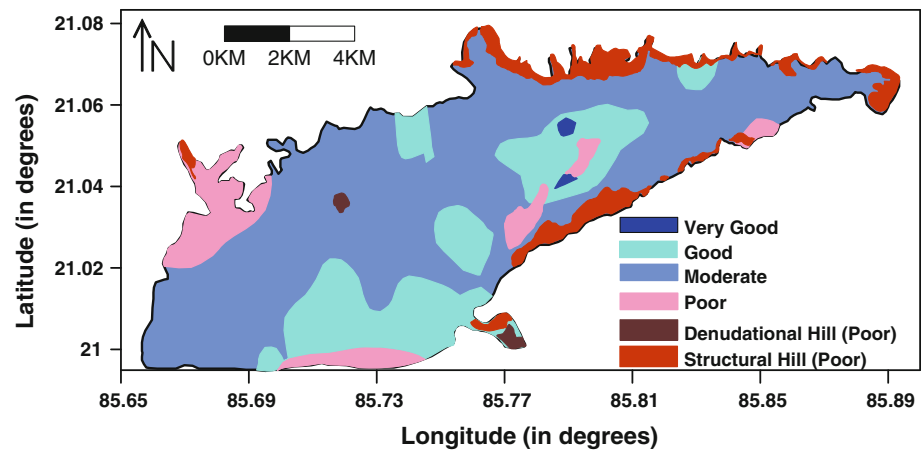
Table 6 Criteria for selecting groundwater prospects map using lineament density and shallow and deeper aquifer thickness

S. no.	Lineament density (m/m^2)	Shallow aquifer thickness (m)	Deeper aquifer thickness (m)	Groundwater prospects
1	>1.5	>15	>15	Very good
2	1.0–1.5	10–15	10–15	Good
3	0.5–1.0	5–10	5–10	Moderate
4	<0.5	<5	<5	Poor

area that shows aquifer thickness more than 15 m is classified as very good for groundwater prospecting.

Groundwater prospects map

The groundwater prospects are much more complicated in hard rock areas especially in areas where different rock formation present. This is true because the deeper aquifers in hard rock terrains are potential only when they are fed by fractures. As of now, there are no satisfactory geological or geophysical techniques to locate the subsurface fractures. The groundwater in the terrain is mostly controlled by the lineaments, fractures and degree of weathering. The lineaments density map as shown in Fig. 6 is superimposed on the map of shallow and deeper aquifer thickness map shown in Fig. 4a, b to decipher new regions of better prospects in the study area, and this map is shown in Fig. 9. Based on lineament density and shallow and deeper aquifer thickness, the groundwater potential map has been classified into four major groups. This classification for obtaining more prominent groundwater prospects map is given in Table 6. This new groundwater prospect map shown in Fig. 9 reveals that areas where the lineament density is high possess thicker aquifer thickness zones and are hence potential regions for prospecting groundwater.

Conclusions

Remote sensing data have been used to interpret the different geomorphological units including structures namely lineaments to identify the zones of groundwater prospects. The various geomorphic units are classified in terms of groundwater prospects, as poor, moderate, good and very good. From VES, it is found that the shallow and deeper aquifer thickness varies spatially and is to some extent controlled by structures. Aquifer is thicker in areas where the lineament density is high, and such regions possess better groundwater potential. The geomorphic regions like valley fills show high degree of weathering. By carrying out comparative study of geomorphic units, lineaments and vertical electrical surveys, one can achieve better results for future groundwater prospects in mining areas, where groundwater is getting declined due to mining. Such study can be important for planning and execution of mining activity. Similarly, comparative study of lineament density and aquifer thickness facilitates delineation of areas of potential groundwater reservoirs, which can be demarcated in the form of maps.

References

Acharya S, Mahalik NK, Mohapatra S (1998) Geology and mineral resources of Orissa, Society of Geoscientists and Allied Technology

Banerjee PK (1971) The Sukinda chromite field, Cuttack dist, Orissa. Rec Geol Surv India 96(Pt.2):140–171

Bhimasankar VLS, Bindi Madhav U, Pantangay NS, Ranga Rao KV (1970) Electrical resistivity investigation for groundwater in parts of Hyderabad district. In: Proceedings of the seminar on incidence of aridity and drought in Andhra Pradesh, Andhra University, Waltair

Bhimasankarm VLS, Gaur VK (1977) Lecture notes on exploration geophysics for geologists and engineers. Association of Exploration Geophysics, Centre for Exploration Geophysics, Hyderabad

Chougule SV (1981) Report on systematic hydrogeological surveys in parts of Salandi-Battarani and Brahmani Basins in Keonjhar, Cuttack and Mayurbhanj dist, Orissa, Un-published CGWB Report

Das S, Kar A (1997) Hydrogeology around Sukinda valley, Orissa with reference to mining activities. Indian J Earth Sci 24(3/4):10–25

Dhakate R, Singh VS, Negi BC, Chandra S, Rao AV (2008) Geomorphological and geophysical approach for locating favorable groundwater zones in granitic terrain, Andhra Pradesh, India. J Environ Manag 88:1378–1383

Dubey N, Trivedi RK (1994) Application of LANDSAT TM imagery and aerial photographs for evaluating the hydrogeological conditions around Damoh, M.P. Bhu-Jal New Faridabad 9(2):1–4

Gajowiec B, Witkowski A (1993) Impact of lead/zinc ore mining on groundwater quality in Trzebionka mine (Southern Poland). Mine Water Environ 12:1–10

Godgul G, Sahu KC (1995) Chromium contamination from chromite mine. Env Geol 25:251–257

Gough LP, Medows GR, Jackson L, Dudken L (1989) Biogeochemistry of highly serpentinized chromite rich ultramafic area, Tahama, County California, US. Geol Surv Bull 1–24

Haridas VK, Chandrasekaran VA, Kumaraswamy K, Rajendran S, Unnikrishnan K (1994) Geomorphological and lineament studies of Kanjamalai using IRS-1 data with special reference to groundwater potentiality. Trans Inst Indian George 16(1):35–41

IBM Publication (1997) Indian mineral book, India, vol 1

Jupp DLB, Vozoff K (1975) Stable iterative methods of inversion of geophysical data. Geophys J RAS, 4 (Implemented by T. Harinarayan on VAX 11/750 at NGRI)

Lokesh KN, Narayana SK (1996) Geomorphological and hydrogeochemical studies of Pangala River basin (D.K), Karnataka. Hydrol J 19(1):33–43

Orellena E, Mooney HM (1966) Master tables and curves for vertical electrical sounding over layered structures. Interciencia, Madrid, Spain, p 150 (66 tables)

Palanivel S, Ganesh A, Vasanthakumaran T (1996) Geohydrological evaluation of upper Agniar and Vellar basins, Tamilnadu: an integrated approach using remote sensing, geophysical and well inventory data. J Ind Soc Remote Sens 24(3):153–168

Rao AV, Dhakate RR, Singh VS, Jain SC (2002) Geophysical and hydrological investigations to delineate aquifer geometry at Kaliapani, Sukinda, Orissa, NGRI Technical Report No. GW-367, pp 1–40

Shahid S, Nath SK (2002) GIS integration of remote sensing and electrical sounding data for hydrogeological exploration. J Spatial Hydrol 2(1):1–12

Sree Devi PD, Srinisasuly S, Kesava Raju K (2001) Hydrogeomophological and groundwater prospects of the Pageru river basin by using remote sensing data. Environ Geol 40:1088–1094

Srivastava PK, Bhattacharya A (2006) Groundwater assessment through an integrated approach using remote sensing, GIS and resistivity techniques: a case study from a hard rock terrain. Int J Remote Sens 27(20/20):4599–4620

Subramanyam V (1986) Lecture notes of short course on the techniques of geomorphologic analyses and application. IIT, Bombay, Mumbai, India (Unpublished)

Teeuw RM (1999) Groundwater exploration using remote sensing and a low-cost geographical information system. Hydrogeol J 3:21–30

Thornburry WD (1969) Principles of geomorphology. Willey, New York

Tiwary RK, Gupta JP, Banerjee NN, Dhar BB (1995) Impact of coal mining activities on water and human health in Damodar River Basin, in: 1st World Mining Environment Congress, New Delhi, India

Yadav GS, Lal T (1989) Investigation of groundwater resources at selected levels in drought prone area of Pahari block, Mirzapur District, UP, India. In: International Workshop Appropriate methodology, Development, Management Groundwater Resources in Developing Countries, vol 1. NGRI, Hyderabad, India, 28 February–4 March 1989, pp 9–219

Zohdy AAR (1974) Application of surface geophysics to groundwater investigations. US Dept. Interior, Geological Survey Book No. 2